Synthesis and some properties of light lanthanide complexes with 4,4′-bipyridine and dibromoacetates

Thermal study

A. Czylkowska

Abstract In this study, new complexes with formulae: Ce(4-bpy)(CHBr$_2$COO)$_3$·H$_2$O, Ln(4-bpy)$_{0.5}$(CHBr$_2$COO)$_3$·2H$_2$O (where Ln(III) = Pr, Nd, Sm; 4-bpy = 4,4′-bipyridine) and Eu(4-bpy)(CHBr$_2$COO)$_3$·2H$_2$O were prepared, and characterized by chemical and elemental analyses, and IR spectroscopy. The way of metal–ligand coordination was discussed. They are small crystalline. The complexes of Pr(III), Nd(III), and Sm(III) are isostructural in group. Conductivity studies (in methanol, dimethylformamide, and dimethylsulfoxide) were also performed and described. The thermal properties of complexes in the solid state were studied using TG–DTG techniques under dynamic flow of air atmosphere. TG–MS system was used to analyze principal volatile thermal decomposition and fragmentation products evolved during pyrolyses of Ce(III) and Sm(III) complexes in dynamic flow of air atmosphere.

Keywords Light lanthanide complexes · 4,4′-Bipyridine · Dibromoacetates · TG–DTG · TG–MS · IR spectra

Introduction

This article is a continuation of our earlier research on lanthanide complexes with 4,4′-bipyridine (4-bpy) and halogenoacetates. The rare earth compounds containing halogenoacetates have been studied by many authors. They consider mainly the metal–ligand coordination and magnetic behavior. The mixed-ligand complexes of some lanthanides with 2,2′- or 4,4′-bipyridine and chloroacetates are known, but with only scant information concerning their

A. Czylkowska (✉)
Institute of General and Ecological Chemistry, Lodz University of Technology, Lodz, Poland
e-mail: agnieszka.czylkowska@p.lodz.pl

thermolysis. Several notes of discussed compounds containing halogenoacetates have been summarized in [1–3].

Our resent investigation related to mixed-ligand lanthanide complexes with 4-bpy and di- or trichloroacetates. We obtained compounds of general formulae: Ln(4-bpy)$_n$(CHCl$_2$COO)$_3$·mH$_2$O [1, 2, 4–7] and Ln(4-bpy)$_n$(CCl$_3$COO)$_3$·mH$_2$O [1, 3, 8, 9] in series Ln(III) = Y, La → Lu (without Pm). They were characterized by elemental analysis, molar conductivity, and IR spectra. Their thermal behaviors were also studied. The way of metal–ligand coordination was discussed. The chloroacetate groups link with rare earth elements in many different ways. In case of La(III) [4] and Sm(III) [5] compounds, dichloroacetate groups coordinate as chelating tridentate and bridging ligands, and in other compounds [2] as bidentate chelating and monodentate ions. In all compounds 4-bpy joins with lanthanide by one nitrogen atom (only in complexes Er(III), Tb(III), and Lu(III), also half molecule of 4-bpy lies in outer coordination sphere [2]). In the literature, there is not much information about lanthanide complexes with bipyridine isomers and dibromoaceates. Thermal studies of compounds with empirical formulae Ln(2-bpy)(CHBr$_2$COO)$_3$·mH$_2$O where Ln(III) = Nd, Er were characterized in [10]. In one of our previous articles, we have described preparation and some behaviors of La(III) and Y(III) complexes with title ligands [11]. In this work, we present the synthesis, some physicochemical properties, and thermal studies of new compounds of light rare earth elements with 4-bpy and dibromoacetates. These studies of lanthanide(III) complexes with 4,4′-bipyridine and halogenoacetates allow us to determinate the influence on the kinds of forming complexes, their properties, and thermal decomposition dependent on the type of halogen atoms in carboxylates.

Experimental

Materials, synthesis, and analysis

4,4'-bipyridine, $CHBr_2COOH$, Ln_2O_3 (where Ln(III) = Nd, Sm, Eu), Pr_6O_{11}, $Ce(NO_3)_3·6H_2O$, dimethylsulfoxide (DMSO), dimethylformamide (DMF), and methanol (MeOH) (anhydrous) p.a. were obtained from Aldrich and Lab-Scan. Water solutions of metal(III) dibromoacetates were prepared by adding 2 mol L^{-1} dibromoacetic acid to freshly precipitated hydroxides (or freshly precipitated cerium(III) carbonate) in ca. stoichiometric quantities. (in temperature ≤18 °C, because lanthanide dibromoacetates in solution are relatively unstable; in presence of 4-bpy their stability arise).

The mixed-ligand complexes were synthesized by reaction of freshly obtained solutions of appropriate Ln(III) dibromoacetaes with solutions of 4-bpy (pH ∼ 5). The molar ratio of M(III):4-bpy was 1:2. Solution of 4-bpy in 31.3 mL of 96 % v/v ethanol (12.4 mmol) was added to 8.7 mL of water solution of Ln(III) dibromoacetates (6.2 mmol). The products were washed in 40 % v/v ethanol and then in ethanol and diethyl ether mixture (1:1). All compounds were dried in open air. The contents of metal(III) ions in obtained solutions were mineralized and determined by EDTA titration.

The carbon, hydrogen, and nitrogen contents in the prepared complexes were determined using a Carbo-Erba analyzer with V_2O_5 as an oxidizing agent.

Methods and instruments

IR spectra were recorded using a NICOLETT 6700 Spectrometer (4000–400 cm^{-1} with accuracy of recording 1 cm^{-1}) using KBr pellets. Molar conductance was measured on conductivity meter of the OK-102/1 type equipped with an OK-902 electrode at 25 ± 0.5 °C, using 1 × 10^{-3} mol L^{-1} solutions of complexes in methanol, dimethylformamide, and dimethylsulfoxide. The thermal properties of complexes in air were studied by TG–DTG techniques in the range of temperature 25–1000 °C at a heating rate of 10 °C min^{-1}; TG and DTG curves were recorded on Netzsch TG 209 apparatus in flow of dynamic

air atmosphere v = 20 mL min^{-1} using ceramic crucibles. The TG–MS coupled measurements have been carried out only for Ce(III) and Sm(III) complexes using the Netzsch TG 209 apparatus coupled with Netzsch MS spectrometer, in the range of temperature of 25–1000 °C at a heating rate 10 °C min^{-1} in flow of air atmosphere v = 20 mL min^{-1} in ceramic crucibles. The m/z values are given based on ^1H, ^{12}C, ^{14}N, ^{16}O, and ^{80}Br (additionally ^{13}C and ^{18}O in case of CO_2). The X-ray powder diffraction patterns of synthesized complexes, and final solid decomposition products in air were recorded on D-5000 diffractometer using Ni-filtered CuK_α radiation. The measurements were carried out in the range of 2θ angles 2°–80°. The obtained results were analyzed using the Powder Diffraction File [12].

Results and discussion

Table 1 presents results of the elemental and chemical analyses of the investigated compounds. They are stable in air in solid state. Single crystals of the investigated complexes were not obtained. The analysis of the X-ray powder diffraction patterns of these compounds reveals that they are small crystalline products and complexes of Pr(III), Nd(III), Sm(III) are isostructural in group. The X-ray powder diffraction patterns of the obtained complexes are not in Powder Diffraction File [12]. Figure 1 presents the X-ray powder diffraction patterns for complexes Ce(III), Pr(III) (as an example of isostructural group), and Eu(III).

The molar conductivities values for complexes in MeOH, DMF, and DMSO are given in Table 1. All complexes in MeOH and DMF display behaviors intermediate between those of non-electrolytes and 1:1 electrolytes. In DMSO they are electrolyte type 1:1 [13]. In series of lanthanide complexes Ce(III) → Eu(III) with 4-bpy and dichloroacetates, the molar conductivities in solutions MeOH, DMF, and DMSO have similar values [6]. Relatively low molar conductances in MeOH and DMF are characteristic for all the complexes compared. They dissociate only to a limited degree in these solutions.

Table 1 Analytical data and molar conductivity in MeOH, DMF, and DMSO for investigated complexes

Compound	Analysis: found (calculated)/%				Λ_M/Ω^{-1} cm^2 mol^{-1}; c = 1 × 10^{-3} mol L^{-1}		
	Ln	C	N	H	MeOH	DMF	DMSO
Ce(4-bpy)$(CHBr_2COO)_3·H_2O$	14.61 (14.52)	20.00 (19.92)	2.82 (2.90)	1.34 (1.36)	51.0	42.0	52.0
Pr(4-bpy)$_{0.5}(CHBr_2COO)_3·2H_2O$	15.49 (15.56)	14.69 (14.60)	1.60 (1.55)	1.21 (1.22)	47.0	47.0	55.0
Nd(4-bpy)$_{0.5}(CHBr_2COO)_3·2H_2O$	15.91 (15.87)	14.46 (14.54)	1.59 (1.54)	1.20 (1.22)	50.3	40.9	51.3
Sm(4-bpy)$_{0.5}(CHBr_2COO)_3·2H_2O$	16.51 (16.43)	14.37 (14.44)	1.51 (1.53)	1.20 (1.21)	45.0	37.4	50.5
Eu(4-bpy)$(CHBr_2COO)_3·2H_2O$	15.37 (15.28)	19.26 (19.32)	2.88 (2.82)	1.31 (1.32)	44.2	36.4	49.8
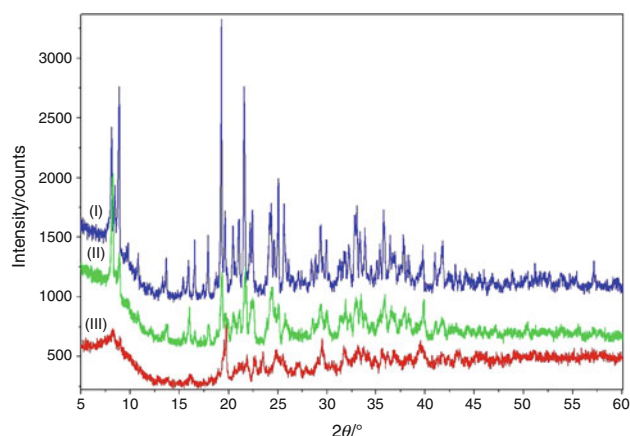
Fig. 1 X-ray powder diffraction patterns for complexes Ce(4-bpy)(CHBr$_2$COO)$_3$·H$_2$O(I), Pr(4-bpy)$_{0.5}$(CHBr$_2$COO)$_3$·2H$_2$O(II) and Eu(4-bpy)(CHBr$_2$COO)$_3$·2H$_2$O(III)

IR spectra

IR spectra of the all fine-crystalline solids show several absorption bands in the region characteristic for dibromoacetates and 4-bpy (Tables 2 and 3). These spectra are very similar, only the asymmetric ν_{as}(COO) band of carboxylate groups in Eu(III) complex is spitted into two clearly separated bands (1706 and 1674 cm^{-1}). In the case of Ce(III), Pr(III), Nd(III), and Sm(III) compounds, the ν_{as}(COO) vibration is identified as the strong band in the range of 1671–1667 cm^{-1}. The band observed at 1386 cm^{-1} has been assigned to the vibration of ν_s(COO) for all complexes. Using the magnitude of $\Delta\nu$ as spectral criterion [16] for determination of mode of bonding carboxylate groups in the obtained compounds, suggest that dibromoacetates in series Ce(III) → Sm(III) act probably as monodentate ligands. The splitting of ν_{as}(COO) band exists in the spectra of Eu(III) compound is probably caused by formation of non-completely equivalent bonds between Eu(III) carboxylate

groups (Table 2) [17, 18]. On the other hand, in all the obtained complexes, the vibrations ν_{as}(COO) and ν_s(COO) are shifted to higher wave numbers corresponding to CHBr$_2$COONa. According to Manhas and Trikha [19] and [20], these bathochromic shifts are evidence leading to the interpretation that the carboxylate groups are bonded to metal(III) as bridging ligands. However, interpretation the nature of bonding lanthanide(III)-carboxylates is difficult. Different types of coordination carboxylate groups to lanthanide ion in one complex and intramolecular hydrogen bonds O(water)-H···O(carboxyl) may exist [2, 4, 5]. In the absorption region of CHBr$_2$COONa appears also the stretching modes ν_s(CBr$_2$) and δ(CCOO). They are in the region of complexes observed between 684–682 cm^{-1} and at 1150 cm^{-1}, respectively. The absorption bands of ν(CH) are in the sodium salt at 3015–1191 cm^{-1}, in the complexes they are in the ranges: 3023–2997 cm^{-1} and 1193–1186 cm^{-1}.

Most bands in the IR spectrum can be attributed to the vibrations of 4-bpy. Their position and tentative assignments for the obtained species are made and given in Table 3. The infrared spectrum of free 4-bpy undergoes a chance upon coordination. The observations were made for 4-bpy absorption in the region 4000–600 cm^{-1}. They are as follows: the band at 1588 cm^{-1} in pure 4-bpy is attributed to the ν(CC), ν(CN), and ν(CC$_{ir}$) vibrations—symmetry A_1, and it shifts toward higher frequency (1612–1607 cm^{-1}). The band in the pure ligand at 1530 cm^{-1}, (ν(CC), and ν(CC) vibrations—symmetry B_1) in the IR spectra of complexes is very small and appears between 1550 and 1520 cm^{-1}. The most characteristic band for 4-bpy is ring "breathing" mode. It shifts toward higher frequencies in comparison with free ligand. The band of free 4-bpy corresponding to ring deformation in plane observed at 608 cm^{-1} shifts to higher frequency after coordination with metal ion. In the regions of bands in the ranges of 1205–1092 and 962–672 cm^{-1}, the spectra of absorption bands for synthesized complexes are poor.

Table 2 IR bands for CHBr$_2$COONa and carboxylate groups in obtained complexes

CHBr$_2$COONa [14]	Complexes					Assignments
	Ce(III)	Pr(III)	Nd(III)	Sm(III)	Eu(III)	
3015	3020	3023	2997	2997	2998	ν(CH)
1616	1667	1667	1669	1671	1706	ν_{as}(COO)
					1674	
1378	1386	1386	1386	1386	1386	ν_s(COO)
1191	1193	1192	1193	1191	1186	ν(CH)
1148	1151	1150	1150	1150	1150	δ(CCOO)
931	955	–	–	–	–	ν(CC)
698	683	683	683	684	682	ν_s(CBr$_2$)
238	282	281	283	285	346	$\Delta\nu = \nu_{as}-\nu_s$
					288	

Table 3 IR bands for free 4-bpy and 4-bpy in obtained complexes

4-bpy [15]	Complexes					Assignments
	Ce(III)	Pr(III)	Nd(III)	Sm(III)	Eu(III)	
1588	1608	1607	1609	1610	1612	$\upsilon(CC)$, $\upsilon(CN)$, $\upsilon(CC_{ir})$, A_1
1530	1533	1530	–	1550	1520	$\upsilon(CC)$, $\upsilon(CN)$ B_1
1488	1490	1490	1490	1490	1489	$\upsilon(CC)$, $\upsilon(CN)$
1403	1413	1415	1413	1415	–	$\upsilon(CC)$, $\upsilon(CN)$
1328	–	–	–	–	–	$\upsilon(CC)$, $\upsilon(CN)$
1205	1226	–	–	–	–	$\beta(CH)$
1092	–	–	–	–	–	$\beta(CH)$
1072	1066	1066	1066	1066	1066	$\beta(CH)$
1037	1043	1045	1040	1040	1043	„ring breathing"
988	1000	1001	1000	999	999	„ring breathing"
962	–	960	–	–	–	$\gamma(CH)$
850	853	850	–	–	–	$\gamma(CH)$
810	809	808	808	808	807	$\gamma(CH)$
745	795	–	–	–	–	$\gamma(CH)$
733	716	716	717	718	718	$\gamma(CH)$
672	–	–	–	–	–	$\gamma(CH)$
608	622	622	623	621	621	$\beta(CH)$
572	596	595	595	595	596	$\beta(CH)$

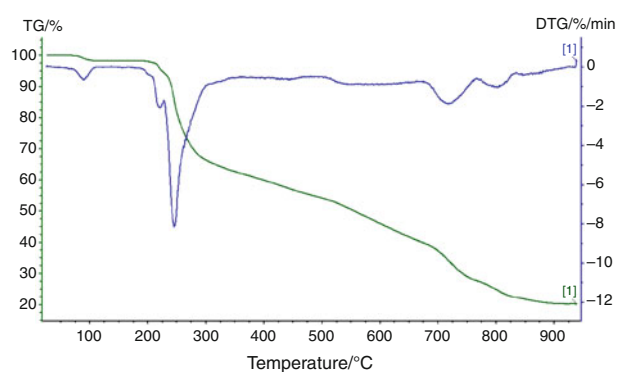*ir* inter ring bands, A_1 symmetry A_1, B_1 symmetry B_1
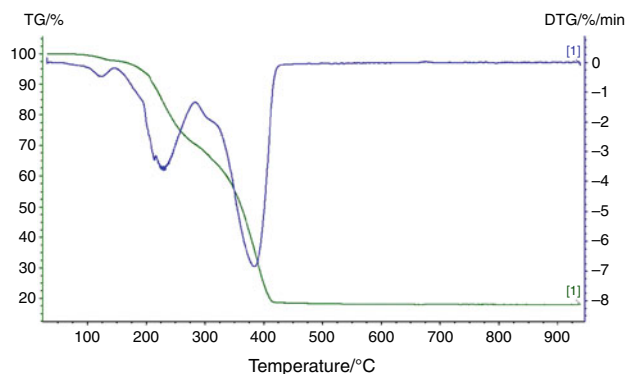
Fig. 2 TG and DTG curves of thermal decomposition of Ce (4-bpy)(CHBr$_2$COO)$_3$·H$_2$O recorded in air atmosphere; mass sample: 9.25 mg

Fig. 3 TG and DTG curves of thermal decomposition of Sm(4-bpy)$_{0.5}$(CHBr$_2$COO)$_3$·2H$_2$O recorded in air atmosphere; mass sample: 6.40 mg

In addition, a broad band in the water stretching region (ca 3450–3350 cm^{-1}) appears for all the described complexes.

Thermogravimetric data in air

The TG–DTG methods were used to describe of thermal decompositions of the obtained complexes in air atmosphere. These thermolyses are complicated and difficult to interpretation. Decomposition of all compounds is multistage and overlapping processes. The first step of pyrolysis is dehydration. When the temperature rises, decomposition of organic ligands begins, and several unidentified solid products are formed. Finally, decomposition products correspond to the suitable oxides. In general, the lines observed for CeO$_2$ and Ln$_2$O$_3$ (Nd, Sm, Eu), Pr$_6$O$_{11}$ correspond to those reported in Powder Diffraction File [12]. Figures 2, 3, and 4 show profiles of TG and DTG of complexes of Ce(III), Sm(III) (as representative specie of isostructural group), and Eu(III). Results of thermal analysis are presented in Table 4.

Ce((4-bpy)(CHBr$_2$COO)$_3$·H$_2$O begins to decompose at 75 °C. It is associated with release water molecule (mass losses calculated 1.87 % and found 1.9 %.). Decomposition of
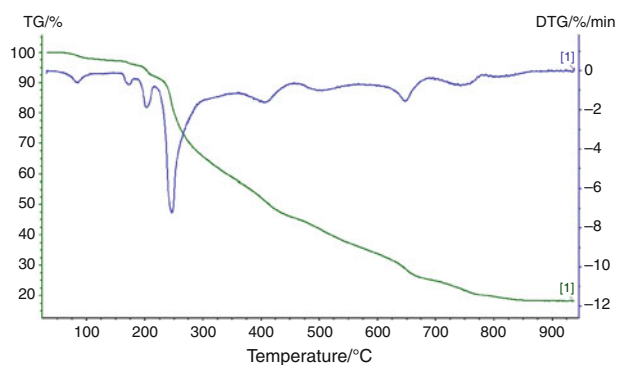
Fig. 4 TG and DTG curves of thermal decomposition of Eu(4-bpy)(CHBr$_2$COO)$_3$·2H$_2$O recorded in air atmosphere; mass sample: 12.96 mg

organic ligands occurs immediately after dehydration at 150 °C. It runs in a few overlapping steps with DTG peak at 230 °C with shoulder at 310 °C. The TG curve shows a rapid mass loss between 150–435 °C and very strong peak 385 °C on DTG curve, as a result of total decomposition of organic ligands. At 435 °C, pure CeO$_2$ is formed as a final product (found: 18.0 %; calc.: 17.84 %).

Complex of Pr(III) dehydrates also in one step in temperature range of 65–150 °C. Above 150 °C, anhydrous unstable complex is formed. After dehydration, further pyrolysis (the destruction of dibromoacetate groups and oxidation of organic fragments) takes place. The DTG curve shows several peaks. A plateau on TG curve begins at 830 °C and corresponds to formation of pure Pr$_6$O$_{11}$ (found: 18.0 %; calc.: 18.80 %).

Nd(III) complex is dehydrated in two steps. At 85 °C, it loses one water molecule. Monohydrate specie is stable up to 175 °C. The next dehydration stage between 175–200 °C takes place. When the temperature is raised further, in TG curve we observe mass loss, which is associated with degradation and combustion of organic ligands. Above 950 °C, Nd$_2$O$_3$ appears very slowly. On DTG curve, peaks are observed at 235, 715, and 835 °C.

In the case of Sm(III) compound, the dehydration process occurs in two steps. At 75 °C, one water molecule is released. The second water molecule is not very well seen on TG curve, and so it is not interpreted. In the temperature range of 180–925 °C, further thermolysis of this specie is observed with DTG peaks occurring at 220, 250, 715, and 800 °C. Final solid product of decomposition is Sm$_2$O$_3$.

The complex Eu(4-bpy)(CHBr$_2$COO)$_3$·2H$_2$O loses 1 mol of water above 65 °C. Next, in the range of 165–185 °C, the last water molecule is eliminated. When the temperature increases, the partial and total destructions of organic ligands take place. The DTG curve exhibits peaks at 205, 250, 410, 500, 650, and 750 °C. Horizontal mass level for Eu$_2$O$_3$ begins at 900 °C.

TG–MS study for Ce(III) and Sm(III) complexes in air

To analyze the principal volatile products evolved during the dynamic thermal decomposition and fragmentation processes of Ce(III) and Sm(III) complexes, a couple TG–MS system was used. The determinations were carried out in dynamic air atmosphere.

For Ce(4-bpy)(CHBr$_2$COO)$_3$H$_2$O, major maxima for ion currents are observed in temperature range of 130–400 °C. The first peaks for OH$^+$ and H$_2$O$^+$ ($m/z = 17, 18$) occurs around 135 °C and are connected with the dehydration of complex. Next, the OH$^+$ and H$_2$O$^+$ are produced by oxidation of organic ligands (peaks at 260 and 350 °C). In the

**Table 4** Thermal decomposition data for obtained complexes in air atmosphere

Complex	Temperature range/°C	Principal peaks of DTG temperature/°C	Mass loss/%		Intermediate and final solid products
			Calc.	Fund.	
Ce(4-bpy)(CHBr$_2$COO)$_3$·H$_2$O	75–150	125	1.87	1.9	Ce(4-bpy)(CHBr$_2$COO)$_3$
	150–435	230, 310sh, 385	80.29	80.1	CeO$_2$
Pr(4-bpy)$_{0.5}$(CHBr$_2$COO)$_3$·2H$_2$O	65–150	110	3.98	4.0	Pr(4-bpy)$_{0.5}$(CHBr$_2$COO)$_3$
	150–830	220-230,425, 560, 650, 785	77.22	78.0	Pr$_6$O$_{11}$
Nd(4-bpy)$_{0.5}$(CHBr$_2$COO)$_3$·2H$_2$O	85–135	110	1.98	2.0	Nd(4-bpy)$_{0.5}$(CHBr$_2$COO)$_3$·H$_2$O
	175–200	170sh	1.98	2.0	Nd(4-bpy)$_{0.5}$(CHBr$_2$COO)$_3$
	>950	235, 715, 835	77.53		Nd$_2$O$_3$*
Sm(4-bpy)$_{0.5}$(CHBr$_2$COO)$_3$·2H$_2$O	75–120	85	1.97	2.0	Sm(4-bpy)$_{0.5}$(CHBr$_2$COO)$_3$·H$_2$O
	180–925	220, 250, 715, 800	78.97	78.0	Sm$_2$O$_3$
Eu(4-bpy)(CHBr$_2$COO)$_3$·2H$_2$O	65–110	85	1.81	1.9	Eu(4-bpy)(CHBr$_2$COO)$_3$·H$_2$O
	165–185	175	1.81	1.9	Eu(4-bpy)(CHBr$_2$COO)$_3$
	185–900	205, 250, 410, 500, 650, 750	78.69	78.2	Eu$_2$O$_3$

sh shoulder

* Very slowly
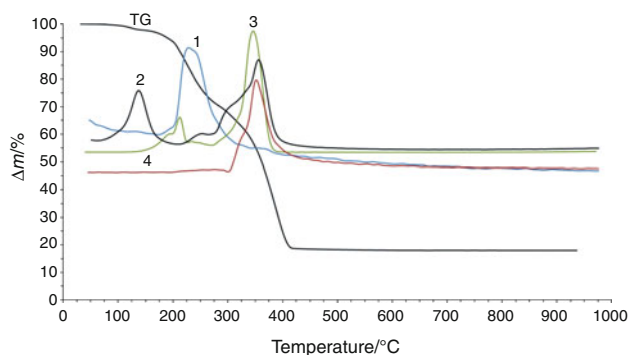
Fig. 5 TG curves for Ce(III) complex and ion current detected by the MS for mass fragments in air; m/z: 1–15; 2–18, 3–44; and 4–80 with sensitivity of ion current: E-9, E-9, E-11, E-12, [A], respectively; mass sample: 8.50 mg
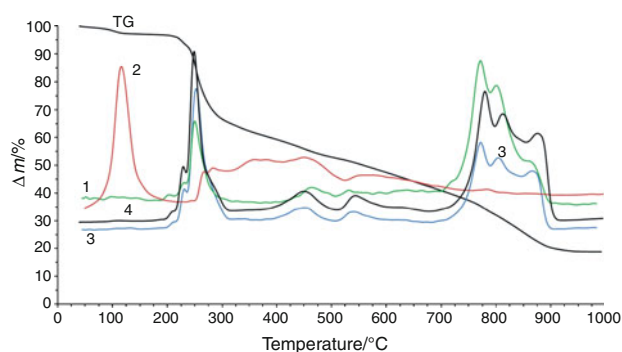
Fig. 6 TG curve for Sm(III) complex and ion current detected by the MS for mass fragments in air; m/z: 1–12; 2–18; 3–30, and 4–44 with sensitivity of ion current: E-9, E-8, E-11, E-9 [A], respectively, mass sample 12.70 mg

range of 190–350 °C, several gaseous products start to liberate. The profiles of CO_2^+ ($m/z = 44, 45, 46$) exhibit maxima at 190°, 210°, and very high intensity at 345 °C. The bromide species: Br^+, HBr^+, CH_2Br^+, and Br_2^+ ($m/z = 80, 93, 94$, and 160, respectively) appear between 230–350 °C. The mass spectrometer detected also the fragments of $m/z = 15$ (CH_3^+ or NH^+), 30 (CH_2O^+ or NO^+), 46 (NO_2^+), 48 ($H_2NO_2^+$), 60 ($C_2H_4O_2^+$), and traces of other ion signals. Maximum rates of formation of CH_3^+ (or NH^+) and CH_2O^+ (or NO^+) are observed at 235 and at 360 °C, respectively. The evaluation of all gaseous products is terminated at about 400 °C. TG–MS data of select ion currents of decomposition for Ce–(III) compound is shown in Fig. 5.

In contrast to the Ce(III) compound, emission of the principal volatile product during thermal decomposition and fragmentation processes for the Sm(III) compound comes to an end at about 900 °C. The peaks of H_2O^+ and OH^+ connected with dehydration occur at about 110 °C. The peaks of these ions appear also in the regions of 255°–510° and 510–775 °C. The ion signal intensities of C^+, CO_2^+, and its

isotopes have centers at 210 °C (very low intensity), 225, 250, 450, 530, 765, 800, and 865 °C; also the profiles of CH_2O^+ or NO^+ ($m/z = 30$) appear. This suggests decomposition and oxidization of organic ligands and the burning of the organic residues. The major ion signals containing bromide: Br^+, HBr^+, CH_2Br^+, and CH_3Br^+ (and its isotopes) have several centers. The first maximum for all these fragments are observed in the temperature range: 235–290 °C. In addition, further maxima of Br^+ ions occur at ca. 460 and 850 °C. The strong peak of CH_3^+ or NH^+ ($m/z = 15$) was monitored at 250 °C. The mass spectrometer detected also the traces of amounts of fragments $m/z = 60$. Figure 6 presents correlation of some ion currents on TG curve of Sm(III) complex in air atmosphere.

Conclusions

On the basis of the present and previous results [4–6], it may be stated that mixed ligand complexes of La(III) and Ce(III) with 4-bpy and dibromoacetates are formed with empirical formulae: Ln(4-bpy)(CHBr$_2$COO)$_3$·H$_2$O. It is similar as was obtained (in the same experimental conditions) in the series of lanthanide(III) complexes Ln(III) = Y, La → Eu (without Pm) with 4-bpy and dichloroacetates [4–6]. On the other hand, the compounds of Pr(III), Nd(III), Sm(III) with 4-bpy and dibromoacetates are of the following type: Ln(4-bpy)$_{0.5}$(CHBr$_2$COO)$_3$·2H$_2$O. The synthesized complexes containing 4-bpy and dibromoacetates are small crystalline. and isostructural in two groups: La(III) [11], Ce(III); and Pr(III), Nd(III), Sm(III).

Changes observed in the IR spectra of complexes indicate that title ligands coordinate to lanthanide ions [2, 4, 5, 16, 21–23]. Probably, the large electronegativity of the substitute bromide atoms in carboxylate group suggests monodentate type of coordination of this ligand.

Thermal decompositions for all the series of discussed compounds in flow of dynamic air atmosphere are of multistage and overlapping processes. The initial temperatures of dehydration processes in the series of lanthanide complexes with 4-bpy and dichloro- or dibromoacetates (where Ln(III) = Y, La → Eu without Pm) do not change regularly with the ionic potential of elements. For compounds Ln(4-bpy)(CHCl$_2$COO)$_3$·H$_2$O (where Ln(III) = Y, La → Eu without Pm) [4–6], the specie of Pr(III) is the least thermally stable. It starts to lose water molecule at 80 °C, where the most stable compound is Eu(4-bpy) (CHCl$_2$COO)$_3$·H$_2$O (100 °C). In the case of lanthanide compounds with 4-bpy and dibromoacetates complex of La(III) [11] is the most stable because its dehydration begins at 100 °C, whereas Y(4-bpy)$_{1.5}$(CHBr$_2$COO)$_3$·3H$_2$O (55 °C) [11] is the least. In general, the obtained results suggest that species including dichloroacetate ligands are

stabler than those containing dibromoacetates. As the final solid products of thermal decomposition are the proper lanthanide oxides.

The TG–MS system was used to determinate volatile products of thermal decomposition of Ce(4-bpy)$(CHBr_2COO)_3 \cdot H_2O$ and Sm(4-bpy)$_{0.5}(CHBr_2COO)_3 \cdot 2H_2O$ complexes in dynamic air atmosphere. The first process is dehydration containing elevation of water. The gas evolved contains ion currents of H_2O^+ and OH^+ ($m/z = 17, 18$). When the temperature rises partial and total decomposition of organic ligands takes place. The major ion signal intensities of H_2O^+, OH^+, C^+, CH_3^+ or NH^+, CO_2^+, and CH_2O^+ or NO^+ appear. In addition, maximum signals containing bromide are observed. Emission of gaseous products in particular steps of thermal decomposition of Ce(III) and Sm(III) complexes correspond with mass losses on TG curves.

References

1. Czylkowska A, Markiewicz M. Coordination behaviour and thermolysis of some rare-earth complexes with 4,4′-bipyridine and di or trichloroacetates. J Therm Anal Calorim. 2010;100:717–23. doi:10.1007/s10973-009-0182-5.

2. Czylkowska A, Czakis-Sulikowska D, Kruszyński R, Markiewicz M. Synthesis, crystal structure and other properties of the complexes of Er(III), Yb(III) and Lu(III) with 4,4′-bipyridine and dichloroacetates. Struct Chem. 2009;21:415–23. doi:10.1007/s11224-009-9545-6.

3. Czylkowska A, Czakis-Sulikowska D, Kaczmarek A, Markiewicz M (2010) Thermal behavior and other properties of Pr(III), Sm(III), Eu(III), Gd(III), Tb(III) complexes with 4,4′-bipyridine and trichloroacetates. J. Therm. Anal. Calorim. doi: 10.1007/s10973-011-1462-4.

4. Czylkowska A, Kruszyński R, Czakis-Sulikowska D, Markiewicz M. Coordination polymer of lanthanum: synthesis, properties and crystal structure of [La(4,4′-bipyridine)(CCl$_2$HCOO)$_3$(H$_2$O)]$_n$. J Coord Chem. 2007;60:2659–69. doi:10.1080/00958970701299550.

5. Kruszyński R, Czylkowska A, Czakis-Sulikowska D. A novel carboxylic coordination polymer of samarium(III): [Sm(H$_2$O)(4,4′-bipyridine)(CCl$_2$HCOO)$_3$]$_n$. J Coord Chem. 2006;59:681–90. doi:10.1080/00958970500345356.

6. Czakis-Sulikowska D, Czylkowska A, Markiewicz M. Synthesis, characterization and thermal decomposition of yttrium and light lanthanides with 4,4′-bipyridine and dichloroacetates. Polish J Chem. 2007;81:1267–75.

7. Czakis-Sulikowska D, Czylkowska A, Markiewicz M, Frajtak M. Synthesis and properties of complexes of Gd(III), Tb(III), Ho(III) and Tm(III) with 4,4′-bipyridine and dichloroacetates. Polish J Chem. 2009;83:1893–901.

8. Czylkowska A. New complexes of heavy lanthanides with 4,4′-bipyridine and trichloroacetates; Synthesis, thermal and other properties. J. Therm. Anal. Calorim. 2012;110:1299–1308.

9. Czylkowska A, Kruszyński R, Kaczmarek A, Markiewicz M. Synthesis and crystal structure of compounds [Ln(H$_2$O)$_8$]$^{3+} \cdot 4CCl_3COO^- \cdot 4H_2O \cdot 2(4$-bpy)$\cdot(4$-bpyH)$^+$. J Chem Struct. 2012;53(5):966–70.

10. Kokonov JV, Segal EJ. Thermal decomposition of complexes of neodynium and erbium with 1,10-phenanthroline and 2,2′-bipyridyl. Rev Roum Chim. 1971;16:1647–50.

11. Czylkowska A, Markiewicz M. Synthesis, thermal behavior and other properties of Y(III) and La(III) complexes with 4,4′-bipyridine and trichloro- or dibromoacetates. J Therm Anal Calorim. 2012. doi:10.1007/s10973-012-2454-8.

12. Powder Diffraction File, PDF-2, release 2004.The International Centre for Diffraction Data (ICDD) 12 Campus Boulevard, Newton Square, PA, USA.

13. Geary WI. The use of conductivity measurements in organic solvents for the characterization of coordination compounds. Coord Chem Rev. 1971;7:81–122. doi:10.1016/S0010-8545(00)80009-0.

14. Spinner E. The vibration spectra of some substituted acetate ions. J Chem Soc. 1964;4217.

15. Pearce CK, Grosse DW, Hessel W. Effect of molecular structure on infrared spectra of six isomers of bipyridine. Chem Eng Data. 1970;15:567–70. doi:10.1021/je60047a042.

16. Nakamoto K. Infrared and Raman spectra of inorganic and coordination compounds. New York: Wiley; 2009.

17. Łyszczek R. Comparison of thermal properties of lanthanide trimellitates prepared by different methods. J Therm Anal Calorim. 2008;93(3):833–8. doi:10.1007/s10973-008-9203-z.

18. Manhas BS, Trikha AK. Relationships between the direction of shifts in the carbon-oxygen stretching frequencies of carboxylato complexes and the type of carboxylate coordination. Indian J Chem. 1982;59:315–9.

20. Ferenc W, Cristóvão B, Sarzyński J, Sadowski P. Complexes of the selected transition metal ions with 4-methoxycinnamic acid. J Therm Anal Calorim. 2012;110:739–48. doi:10.1007/s10973-011-1935-5.

21. Ye HM, Ren N, Li H, Zhang JJ, Sun SJ, Tian L. Synthesis, crystal structure and thermal decomposition kinetics of complex [Nd(BA)$_3$bipy]$_2$. J Therm Anal Calorim. 2010;101:205–11. doi:10.1007/s10973-009-0428-2.

22. Rzączyńska Z, Kula A, Sienkiewicz-Gromiuk J, Szybiak A. Synthesis, spectroscopic and thermal studies of 2,3-naphthalenedicarboxylates of rare earth elements. J Therm Anal Calorim. 2011;103:275–81. doi:10.1007/s10973-010-0927-1.

23. Łyszczek R. Hydrothermal synthesis, thermal and luminescent investigations of lanthanide(III) coordination polymers based on the 4,4′-oxybis(benzoate) ligand. J Therm Anal Calorim. 2012;108:1101–10. doi:10.1007/s10973-011-1987-6.